

# The Effects of Orbital Environment on X-ray CCD Performance

Catherine E. Grant, Beverly LaMarr, Eric D. Miller, and Marshall W. Bautz

Kavli Institute for Astrophysics and Space Research, Massachusetts Institute of Technology, Cambridge, MA 02139, USA e-mail: cgrant@space.mit.edu

## ABSTRACT

*Context.* The performance of CCD detectors aboard orbiting X-ray observatories slowly degrades due to accumulating radiation damage.

*Aims.* In an effort to understand the relationship between CCD spectral resolution, radiation damage, and the on-orbit particle background, we attempt to identify differences arising in the performance of two CCD-based instruments: the Advanced CCD Imaging Spectrometer (ACIS) aboard the Chandra X-ray Observatory, and the X-ray Imagine Spectrometer (XIS) aboard the Suzaku X-ray Observatory.

*Methods.* We compare the performance evolution of front- and back-illuminated CCDs with one another and with that of very similar detectors installed in the ACIS instrument aboard Chandra, which is in a much higher orbit than Suzaku. We identify effects of the differing radiation environments as well as those arising from structural differences between the two types of detector.

*Results.* There are some differences and these are they.

**Key words.** some keywords

## 1. Introduction

- summary of usage of CCDs in X-ray instruments (ASCA, Chandra, XMM, Suzaku) and why they're good
  - large field of view
  - high sensitivity
  - broad energy range
  - moderate spectral resolution
- effects of radiation damage; specifically soft proton damage to ACIS
  - production of charge traps leads to increased CTI
  - increased FWHM, decreased gain
- mitigation by sacrificial charge
  - background events fill traps on readout
  - charge injection fills traps on readout
- thus the response of a CCD-based instrument is largely determined by its particle environment
  - differences in orbit can be used to produce a model of the interplay between particle background and changes in the spectral resolution
  - ACIS and XIS have similar CCDs in very different orbits
  - more than 18 years of monitoring data from ACIS and XIS combined

## 2. Description of the Instruments

### 2.1. CCD Detector Characteristics

The CCD chips in ACIS and the XIS were fabricated at MIT Lincoln Laboratory and are very similar in design.

Chandra has a single X-ray telescope and a moveable Science Instrument Module (SIM), upon which ACIS is mounted. The ACIS focal plane consists of ten CCD devices (model CCID17), eight of which are front-illuminated (FI) and two of which are back-illuminated (BI). The layout of the ACIS devices is shown in Figure 1. The CCD characteristics are summarized in Table 1 and described in detail by Garmire et al. (2003).

Suzaku has four XIS instruments, each with an independent X-ray Telescope (XRT) and focal plane assembly. The four devices are model CCID41, comprising three FI chips (XIS0, XIS2, and XIS3) and one BI (XIS1). One of the FI devices (XIS2) was damaged by a likely micrometeorite strike in October 2006 and has been unused since that time. The CCDs are summarized in Table 1 and described in detail by Koyama et al. (2007). The XIS devices are physically very similar to the ACIS devices with one notable exception, the addition of charge injection capabilities in the XIS CCID41 (Bautz et al. 2007). This is described in further detail in Section ??.

### 2.2. Orbital Radiation Environments

- ACIS
  - elliptical, 2.5 day orbit
  - initial 8 rad belt passages
    - weakly penetrating trapped soft protons 0.1-0.5 MeV (O'Dell et al. 2000)
    - only damaged FIs, through damage to buried channel
  - ongoing radiation damage

- weakly penetrating soft protons focussed by HRMA
- strongly penetrating solar protons and cosmic rays passing through shielding
- XIS
  - low-earth, 90 minute orbit
  - 30 degree inclination
    - SAA passages

### 3. Methodology

#### 3.1. Data and Analysis

- description of the data used
- description of the processing done

#### 3.2. A Proxy for Measuring CTI

A proper measurement of parallel CTI requires full illumination of the CCD with a source of known energy. ACIS is equipped with an External Calibration Source (ECS) comprising a  $^{55}\text{Fe}$  source and aluminum and titanium targets that is capable of illuminating the entire CCD array with photons at a number of specific energies. The XIS instruments have fixed  $^{55}\text{Fe}$  sources that illuminate the two corners farthest from the readout of each CCD with photons from Mn  $K\alpha$  (5.9 keV) and Mn  $K\beta$  (6.5 keV). Since the XIS calibration sources are incapable of illuminating the full chip, for proper comparison we must restrict our analysis to the upper corners of the ACIS chips as well. A change in CTI must change the accumulated charge loss and thus the pulseheight far from the framestore region. A change in pulseheight, however, does not necessarily have to be related to CTI; it could also be due to a changes in the gain completely unrelated to radiation damage.

ACIS has a known slow change in the gain as a function of time as measured very close to the framestore where CTI should be negligible. For all of the CCDs except I0 and I2 it is monotonically decreasing at a rate of  $\sim 1 \text{ ADU yr}^{-1}$  at 5.9 keV.<sup>1</sup> (The gain changes on I0 and I2 are pathological with jumps and annual trends that are irrelevant to the CTI proxy analysis at hand, so they are excluded here.)

To determine the feasibility of using only the upper corners as a CTI metric, we compared the change in Mn  $K\alpha$  pulseheight to the measured CTI for two ACIS chips. The results are shown in Figure 2. Prior to correcting for the known gain change, the fractional pulseheight change is well-correlated to the CTI (left panels). After the correction, the correlation is even tighter (right panels). The correction coefficient was fit by eye, finding the value the best reduced the ACIS-I3 scatter. The correction is always less than 0.5% of the total pulseheight.

- how relevant is this to XIS?

### 4. Discussion

#### 4.1. CTI Time Evolution

##### 4.1.1. Front- vs. Back-Illuminated Detectors

##### 4.1.2. Chandra vs. Suzaku

#### 4.2. Charge Trailing Time Evolution

#### 4.3. Spectral Resolution Time Evolution

##### 4.3.1. Front- vs. Back-Illuminated Detectors

##### 4.3.2. Chandra vs. Suzaku

#### 4.4. CTI and Spectral Resolution: Dependence on Background

### 5. Conclusions

*Acknowledgements.* The authors thank blah blah and blah blah for such and such. This work was supported by NASA grant so and so.

### References

- Bautz, M. W., LaMarr, B. J., Miller, E. D., et al. 2007, in Society of Photo-Optical Instrumentation Engineers (SPIE) Conference Series, Vol. 6686, Society of Photo-Optical Instrumentation Engineers (SPIE) Conference Series
- Garmire, G. P., Bautz, M. W., Ford, P. G., Nousek, J. A., & Ricker, Jr., G. R. 2003, in Society of Photo-Optical Instrumentation Engineers (SPIE) Conference Series, Vol. 4851, Society of Photo-Optical Instrumentation Engineers (SPIE) Conference Series, ed. J. E. Truemper & H. D. Tananbaum, 28–44
- Koyama, K., Tsunemi, H., Dotani, T., et al. 2007, PASJ, 59, 23

<sup>1</sup> See <http://space.mit.edu/cgrant/gain> and <http://space.mit.edu/cgrant/line> for example plots of the gain change.

# ACIS FLIGHT FOCAL PLANE

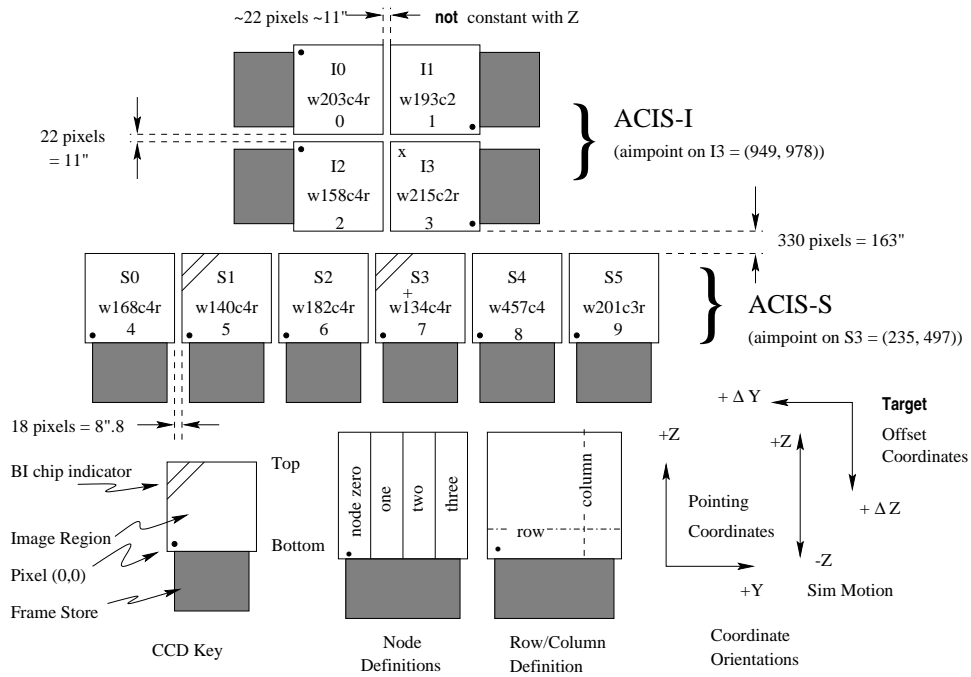


Fig. 1. Schematic drawing of the ACIS focal plane, from the Chandra Proposer's Observatory Guide.

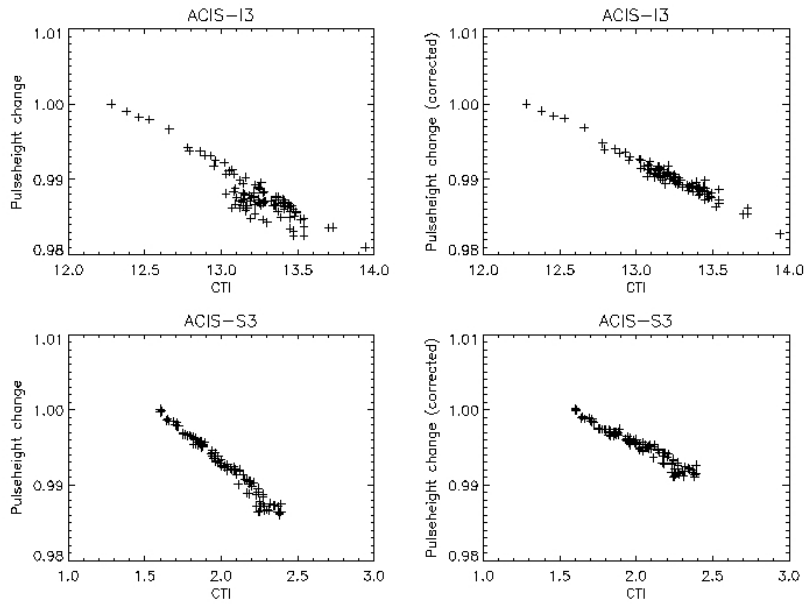
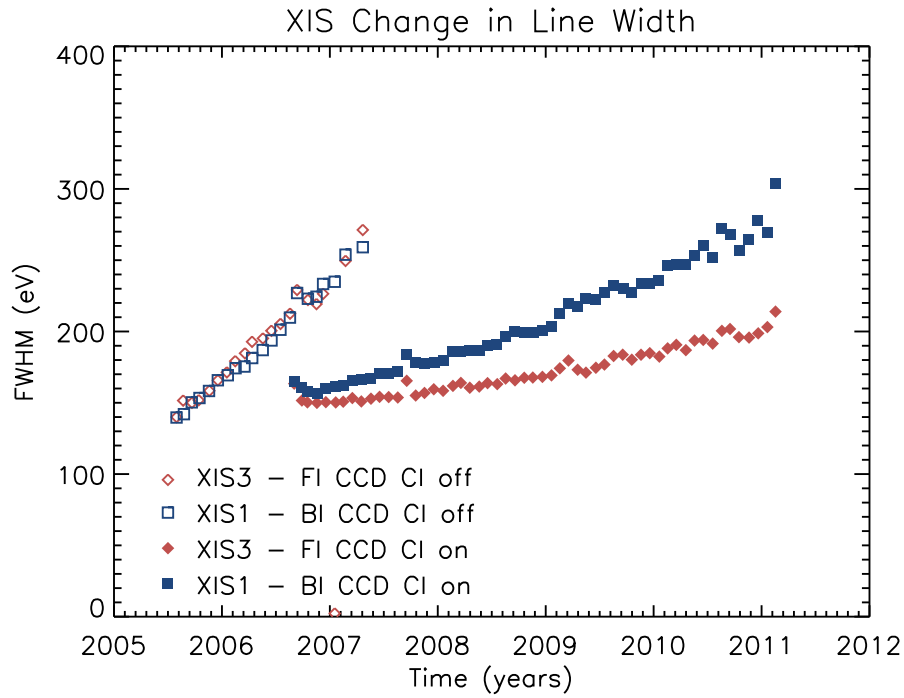
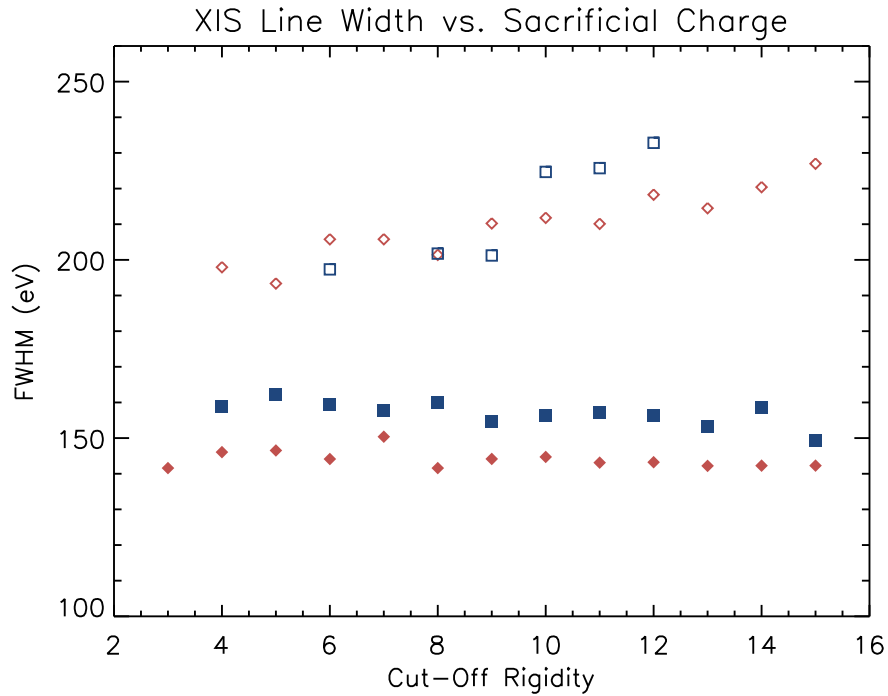


Fig. 2. CTI ( $\times 10^5$ ) versus the fractional change in Mn  $K\alpha$  pulseheight for two ACIS devices, I3 (FI) and S3 (BI), as measured from the upper corners of each chip. The left panels show the measured data, while the right panels show data corrected for a slow gain decrease, discussed in the text. The CTI and pulseheight are well-correlated.



**Fig. 3.** Change in XIS line width (FWHM) with time over the course of the *Suzaku* mission, as measured at Mn  $K\alpha$ . Different symbols show FI and BI devices with charge injection (CI) on and off.



**Fig. 4.** XIS Mn  $K\alpha$  line width (FWHM) as a function of the geomagnetic cut-off rigidity (COR), averaging over the course of the mission. Symbols are the same as in Figure 3. Lower cut-off rigidity indicates a higher particle background, therefore the narrower line widths at low COR in the FI, CI off data (open points) are due to sacrificial charge. Use of CI overwhelms the effects of sacrificial, charge, so no dependence on COR is seen in those data (solid points).

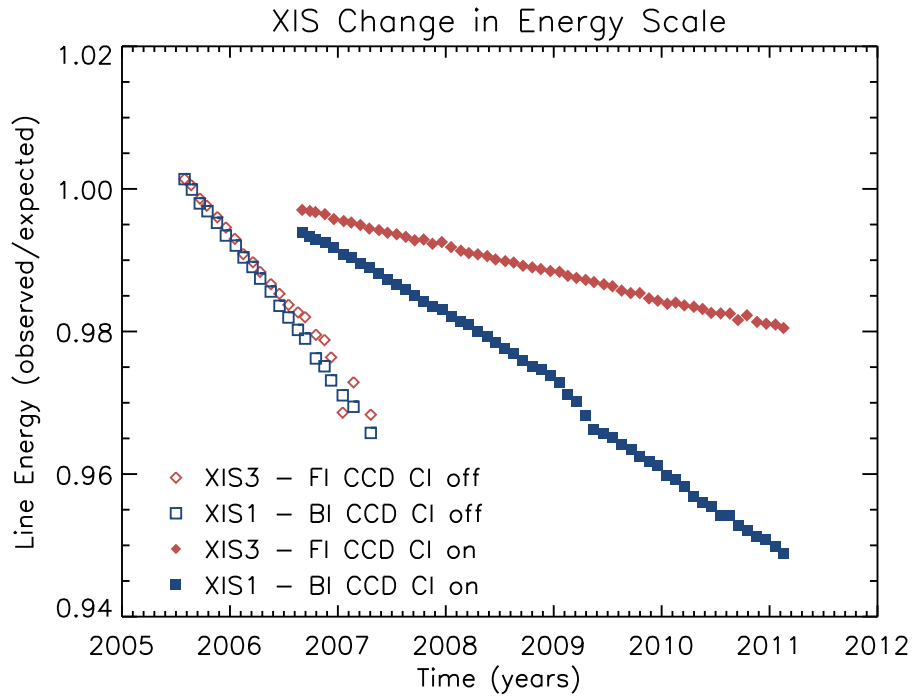


**Fig. 5.** Fractional change in the measured XIS central line energy over the course of the *Suzaku* mission, as measured at Mn  $K\alpha$ . Different symbols show FI and BI devices with charge injection (CI) on and off.

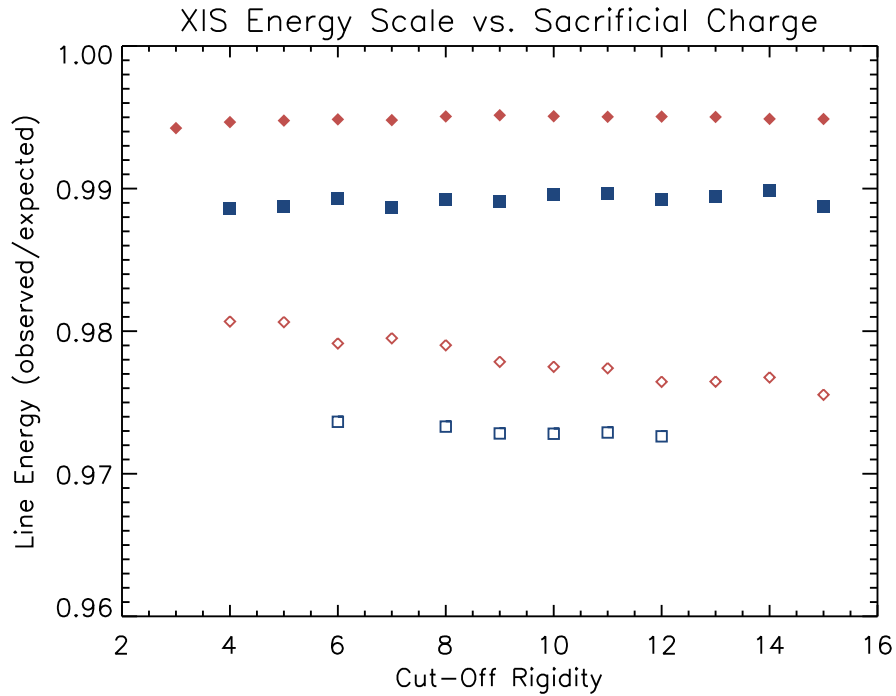


**Fig. 6.** Fractional change in the XIS line energy as a function of COR, averaging over the course of the *Suzaku* mission. Symbols are the same as in Figure 5. A trend toward lower line energy (increased CTI) with higher COR (decreased background) is seen in the FI, CI off data. This results from lower amounts of sacrificial charge. As with the line width in Figure 4, use of CI overwhelms the effects of sacrificial charge (solid points).

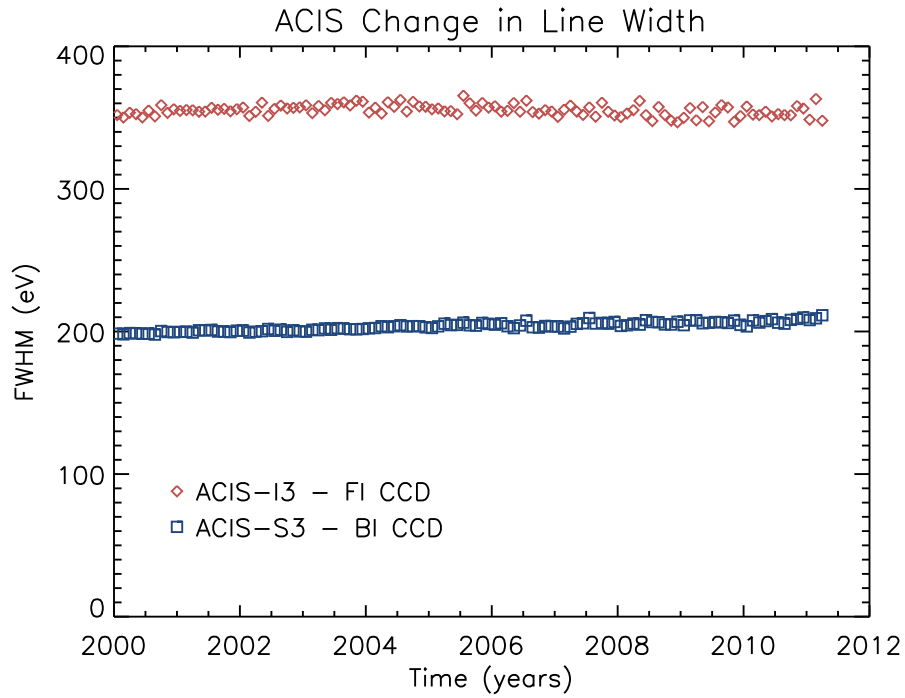


**Fig. 7.** Change in ACIS line width over the course of the *Chandra* mission, as measured at Mn  $K\alpha$ .

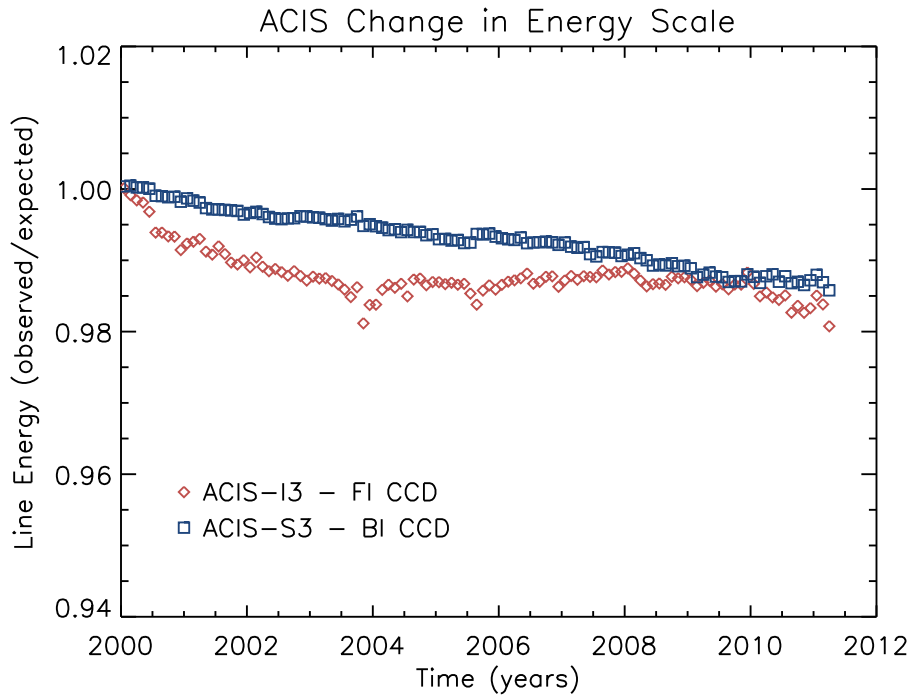


**Fig. 8.** Fractional change in ACIS line central energy over the course of the *Chandra* mission, as measured at Mn  $K\alpha$ . The effects of varying partial background and sacrificial charge are seen in the ACIS-I3 (FI) data.

**Table 1.** Characteristics of MIT Lincoln Laboratory CCDs for ACIS and XIS

	ACIS	XIS
Model	CCID17	CCID41
Format	1026 rows $\times$ 1024 pixels/row (imaging area)	
Architecture	3-phase, frame-transfer, four parallel output nodes	
Illumination Geometry	8 FI & 2 BI	2 FI & 1 BI
Charge Injection Capable	no	yes
Pixel Size	24 $\times$ 24 $\mu\text{m}$	
Readout Noise (RMS)	2–3 $e^-$ at 400 kpix $s^{-1}$	< 2.5 $e^-$ at 41 kpix $s^{-1}$
Depletion Depth	FI: 64–76 $\mu\text{m}$ ; BI: 30–40 $\mu\text{m}$	FI: 60–65 $\mu\text{m}$ ; BI: 40–45 $\mu\text{m}$
Operating Temperature	–120°C via radiative cooling	–90°C via Peltier cooler
Frame Exposure Time <sup>a</sup>	3.2 s	8.0 s
Pre-Launch CTI ( $10^{-5}$ )	FI: ??? BI: ???	FI: ??? BI: ???

<sup>(a)</sup> In normal operating mode.